

**FABRICATION, CHARACTERIZATION AND APPLICATION
OF POLYHYDROXYBUTYRATE-TITANIUM DIOXIDE
NANOCOMPOSITE MATERIALS**

by

NANTHINI SRIDEWI A/P APPAN

**Thesis submitted in fulfillment of the requirements
for the degree of
Doctor of Philosophy**

February 2012

ACKNOWLEDGEMENTS

First and foremost, I offer my sincerest gratitude to my supervisor, Prof. Dr. K. Sudesh Kumar, who has supported me throughout my research with his constructive suggestions, patience and knowledge.

I am truly grateful to Prof. T. T. Teng from the Environmental Technology Division, School of Industrial Technology and Prof. Zairi Jaal from the Vector Control Research Unit, School of Biological Sciences for allowing me to learn and use the facilities in their respective laboratories. I also thank Mr. R. Patchamuthu and Ms. Jamilah Afandi of Electron Microscopy Unit, School of Biological Sciences during SEM analyses and Mr. M. Nasir Hasan from the Vector Control Research Unit for his technical assistance in mosquito larval bioassay during my research.

Not to forget, all the members of Ecobiomaterial Lab who had been both encouraging and inspiring in many ways.

My deepest gratitude goes to my parents, brothers, sisters and niece for their unconditional love, understanding and belief on me thus far. My special thanks go to my husband, Karthik whom had always been there for me through thick and thin and supported me emotionally.

I would like to express my appreciation to Ministry of Science and Technology (MOSTI) for the financial support through National Science Foundation Fellowship.

Lastly, I thank GOD for his blessings and the wonderful experience he had granted me.

TABLE OF CONTENTS

ACKNOWLEDGEMENT	ii
TABLE OF CONTENTS	iii
LIST OF TABLES	ix
LIST OF FIGURES	x
LIST OF PLATES	xv
LIST OF ABBREVIATIONS	xvi
ABSTRAK	xviii
ABSTRACT	xx
1.0 INTRODUCTION	1
1.1 Research objectives	5
2.0 LITERATURE REVIEW.....	7
2.1 Overview of polyhydroxyalkanoate (PHA).....	7
2.2 PHA biosynthesis	10
2.3 Poly(3-hydroxybutyrate), (3HB)	13
2.4 Poly(3-hydroxybutyrate-co-3-hydroxyvalerate), P(3HB-co-3HV)	15
2.5 Poly(3-hydroxybutyrate-co-3-hydroxyhexanoate), P(3HB-co-3HHx)	16
2.6 Extracellular PHA degradation.....	17
2.7 Dye wastewater	19
2.7.1 Types of dyes.....	20
2.8 An outlook on the current wastewater treatment methods	22
2.8.1 Coagulation/flocculation	22
2.8.2 Filtration	23
2.8.3 Adsorption	24
2.8.4 Biological treatment	26
2.9 Advanced oxidation process (AOP)	27

2.9.1	Characteristics of TiO ₂ photocatalyst	27
2.9.2	Mechanism of TiO ₂ photocatalysis	28
2.9.3	Immobilization of TiO ₂ photocatalyst	30
2.10	Batik dye.....	33
2.11	Malachite Green	35
2.12	Electrospinning.....	37
2.12.1	Electrospinning of TiO ₂ nanofibers	40
3.0	METHODOLOGY	42
3.1	Chemicals	42
3.2	General methods	42
3.3	Procurement of PHA polymers	43
3.3.1	Biosynthesis of P(3HB- <i>co</i> -5 mol% 3HHx)	43
3.3.2	Maintenance of the bacterial strain.....	43
3.3.3	Biosynthesis of P(3HB- <i>co</i> -5 mol% 3HHx) via one-stage cultivation..	44
3.3.4	Phase contrast microscopy analysis	45
3.3.5	Determination of PHA content and composition by using gas chromatography (GC)	45
3.3.5 (a)	Preparation of methanolysis solution	46
3.3.5 (b)	Preparation of CME (caprylate methyl ester) solution	47
3.3.6	Polymer extraction	47
3.3.7	Purification of P(3HB)	47
3.3.8	Preparation of PHA and PHA-TiO ₂ based nanocomposite films for degradation studies Polymer extraction	48
3.4	Assessment of the degradation of PHAs and PHA-TiO ₂ based films in a mangrove environment	49
3.4.1	Experimental designs and sampling gears.....	49
3.4.2	Determination of biodegradation.....	51

3.4.3	Molecular weight determination.....	51
3.4.4	Microbial enumeration	52
3.4.5	Observation of surface morphology changes via scanning electron microscopy (SEM) and stereo microscopy	53
3.5	Decolorization studies using cast films	53
3.5.1	Wastewater samples	53
3.5.2	Preparation of P(3HB)-TiO ₂ nanocomposite films for decolorization studies	54
3.5.3	Photocatalytic decolorization experiment using P(3HB)-TiO ₂ nanocomposite films	56
3.5.4	Evaluation of COD removal in Batik dye wastewater treated using P(3HB)-TiO ₂ nanocomposite films	56
3.5.5	Scanning electron microscopy (SEM).....	57
3.5.6	Toxicity test of the Batik dye wastewater using microalgae.....	57
3.5.7	Toxicity test of the Batik dye wastewater using mosquito larvae.....	58
3.6	Decolorization studies using electrospun films.....	59
3.6.1	Fabrication of P(3HB) and P(3HB)-TiO ₂ electrospun films	59
3.6.2	Fabrication of P(3HB) and P(3HB)-TiO ₂ solvent cast films for MG decolorization experiment	60
3.6.3	Qualitative characterization of electrospun fibers.....	61
3.6.4	Energy dispersive X-ray (EDX) Analysis	61
3.6.5	Decolorization of MG via adsorption, photocatalytic degradation and photolysis	62
3.6.6	Evaluation of COD removal in MG treated using P(3HB)-TiO ₂ nanocomposite films	62
3.6.7	Toxicity evaluation on MG treated using P(3HB)-TiO ₂ nanocomposite films	63

3.7	Effect of light sources on the photocatalytic activity for bacterial killing	63
3.8	Statistical analysis	64
4.0	RESULTS	65
4.1	Effect of zonal variation on the overall degradation of PHAs and PHA-TiO ₂ based material in a mangrove environment	65
4.2	Microbial enumeration of surface sediment samples using modified marine agar	73
4.3	Degradation trend of P(3HB) and its copolymers in mangrove sediment	75
4.4	Optimization of system and process parameters for the development of P(3HB)-TiO ₂ nanocomposite film	81
4.4.1	Effect of the initial concentration of methylene blue on the decolorization efficiency of P(3HB)-TiO ₂ nanocomposite film	81
4.4.2	Effect of fabrication method of P(3HB)-TiO ₂ composite film on its decolorization efficiency	83
4.4.3	Effect of P(3HB)-TiO ₂ nanocomposite film thickness on the decolorization efficiency of methylene blue	87
4.4.4	Effect of TiO ₂ concentrations in P(3HB) films on dye decolorization	89
4.5	Decolorization of real industrial Batik dye wastewater using 0.4 g P(3HB)-40 wt% TiO ₂ film	91
4.6	Re-applicability of 0.4 g P(3HB)-40 wt% TiO ₂ film in Batik dye wastewater decolorization	93
4.7	Effect of different pH of Batik dye wastewater on the decolorization efficiency	96
4.8	COD removal in Batik dye wastewater via treatment using 0.4 g P(3HB)-40 wt% TiO ₂ film	98
4.9	Evaluation of the toxic effects of Batik dye wastewater using organisms of different trophic levels	100

4.9.1 Toxicity evaluation of Batik wastewater using <i>S. quadricauda</i> as a bioindicator	100
4.9.2 Toxicity evaluation of Batik wastewater using <i>A. aegypti</i> as a bioindicator.....	102
4.10 Electrospinning as means of producing P(3HB)-TiO ₂ nanofibers.....	105
4.10.1 Effect of CHCl ₃ neat solvent on the electrospinnability of P(3HB).....	105
4.10.2 Effect of CHCl ₃ /DMF mixed solvent on the electrospinnability of P(3HB).....	110
4.11 Electrospinning of P(3HB)-TiO ₂ nanocomposite fibers	112
4.12 Effect of CHCl ₃ /DMF ratio on the morphology of electrospun P(3HB)-50 wt% TiO ₂ fibers	117
4.13 Effect of applied voltage on the morphology of electrospun P(3HB)-50 wt% TiO ₂ fibers	120
4.14 Decolorization of Malachite green using electrospun and cast P(3HB) and P(3HB)-50 wt% TiO ₂ films	123
4.14.1 Dye Adsorption analysis.....	123
4.14.2 Photolysis and photocatalytic decolorization of MG under various light sources.....	127
4.15 COD removal in Malachite green solution after treatment with electrospun P(3HB)-50 wt% TiO ₂ film	131
4.16 Evaluation of the toxic effects of MG solution using <i>A. aegypti</i>	133
4.17 Studies on the re-applicability of P(3HB)-TiO ₂ films.....	135
4.18 Bactericidal assessment on cast and electrospun P(3HB)-50 wt% TiO ₂ fiber.....	140
5.0 DISCUSSION.....	142
6.0 CONCLUSION	188
7.0 RECOMMENDATIONS FOR FUTURE STUDIES.....	192

REFERENCES	193
APPENDICES	220
LIST OF PUBLICATIONS AND CONFERENCE PRESENTATIONS	228

LIST OF TABLES

	Page
2.0 Literature Review	
Table 2.1	Classification of dyestuffs 21
Table 2.2	Summary of catalyst supports for the immobilization of TiO ₂ in heterogeneous photocatalysis 32
3.0 Methodology	
Table 3.1	Characteristics of Batik dye wastewaters collected from small-scale and medium-scale Batik operations located in Penang, Malaysia 55
4.0 Results	
Table 4.1	Physico-chemical characteristics of three study zones assigned at the mangrove compartment of Sungai Pinang, Penang 69
Table 4.2	Changes in M_n and polydispersity values of P(3HB), P(3HB-co-5 mol% 3HV) and P(3HB-co-5 mol% 3HHx) films on the sediment surface ^a during the first 3 weeks of the degradation study 80
Table 4.3	Decolorization ¹ percentage of different concentrations of methylene blue using P(3HB)-TiO ₂ films of different thickness 82
Table 4.4	Decolorization ¹ percentage of methylene blue using different concentrations of TiO ₂ in 0.4 g P(3HB)-TiO ₂ films 90
Table 4.5	Repeated usage of 0.4g P(3HB)-40 wt% TiO ₂ films in the decolorization ¹ of Batik dye wastewater 94
Table 4.6	The effect of pH value on the decolorization ¹ percentage of batik dye wastewater using 0.4g P(3HB)-40 wt% TiO ₂ 97
Table 4.7	Energy dispersive X-ray (EDX) analysis of electrospun and cast P(3HB)-50 wt% TiO ₂ composite films 124
Table 4.8	Energy Dispersive X-ray (EDX) analysis on electrospun P(3HB)-50 wt% TiO ₂ and cast P(3HB)-50 wt% TiO ₂ composite films after usage in ten repeated decolorization experiments 139

LIST OF FIGURES

	Page
2.0 Literature Review	
Figure 2.1	General structures of polyhydroxyalkanoates. 9
Figure 2.2	Biosynthesis pathway of (A) P(3HB); (B) P(3HB)- <i>co</i> -(3HV); (C) P(3HB)- <i>co</i> -(3HHx) via fatty acid β -oxidation and (D) P(3HB)- <i>co</i> -(3HHx) via fatty acid <i>de novo</i> synthesis. 11
Figure 2.3	Schematics of the electrospinning experimental set up of (A) vertical and (B) horizontal geometry. 39
3.0 Methodology	
Figure 3.1	Schematics showing the deployment of PHA and PHA-TiO ₂ nanocomposite film samples and sampling gears in mangrove sediment. 50
4.0 Results	
Figure 4.1	Schematics showing the locations of the three study stations indicated as (I) zone I; (II) zone II and (III) zone III in an intermediate mangrove compartment along Sungai Pinang, west of Penang Island. 67
Figure 4.2	Weight loss profile of P(3HB) and P(3HB)-TiO ₂ films on the sediment surface at (A) zone I; (B) zone II and (C) zone III over a period of 8 weeks in the mangrove compartment of Sungai Pinang. 71
Figure 4.3	Weight loss profile of P(3HB) and P(3HB)-TiO ₂ films buried in the sediment at (A) zone I; (B) zone II and (C) zone III over a period of 8 weeks in the mangrove compartment of Sungai Pinang. Test samples were buried at a depth of 20 cm from the sediment surface. 72
Figure 4.4	Microbial population in the sampling zones expressed as average log ₁₀ (CFU/mL) counts. The sediment samples of (A) zone I; (B) zone II and (C) zone III were inoculated on different agar media and incubated at 30 °C for 24 h. 74
Figure 4.5	SEM micrographs showing the morphology changes in the surface of buried PHA films exposed to degradation. The porosity of (A-C) P(3HB); (D-F) P(3HB)- <i>co</i> -5 mol% 3HV) and (G-I) P(3HB)- <i>co</i> -5 mol% 3HHx) was found to increase with incubation time of the films. 76

Figure 4.6	SEM micrographs showing the colonization of various microorganisms on the surface of (A) & (B) P(3HB); (C) & (D) P(3HB-co-5 mol% 3HV) and (E) & (F) P(3HB-co-5 mol% 3HHx) films at fourth week of incubation in mangrove sediment. Bacteria with coccal morphology were seen attached to the PHA surface in (A) and (F). Pennate diatoms were found to colonize the film surface in (B) and (D). In (C), arrows indicate the growth of pseudo-hyphae structures on the film surface whereas hemispherical cavities caused by bacterial degradation are indicated by arrows in (E).	77
Figure 4.7	Degradation illustrated by physical changes in the buried PHA films over the first 6 weeks of the degradation experiment at zone III. Films shown represent the changes in films retrieved from three sampling points at zone III.	78
Figure 4.8	The decolorization percentage of methylene blue [0.01 mM] over time using P(3HB)-TiO ₂ films fabricated via Method A and Method B. Decolorization experiments were carried out for 3h under solar irradiation with an intensity range of 77,800-85,000 Lux.	84
Figure 4.9	SEM micrograph showing the surface morphology of P(3HB)-TiO ₂ composite films prepared using (a) Method A and (b) Method B. The films were prepared by conventional solvent-cast technique.	86
Figure 4.10	The decolorization percentage of methylene blue [0.01 mM] over time using P(3HB)-TiO ₂ films of varied thickness at fixed amount of TiO ₂ (0.27 g). Decolorization experiments were carried out for 3h under solar irradiation with an intensity range of 85,400-90,100 Lux.	88
Figure 4.11	The decolorization percentage of dye wastewater obtained from a medium scale Batik industry over time using 0.4 g P(3HB)-40 wt% TiO ₂ films. Decolorization experiments were carried out for 3h under solar irradiation with an intensity range of 85,100-89,500 Lux.	92
Figure 4.12	COD reduction in Batik dye wastewater over time via photocatalytic degradation using cast P(3HB)-40 wt% TiO ₂ film. The solar light intensity during triplicate experiments was in the range of 85,100-89,500 Lux.	99
Figure 4.13	Survival of <i>Scenedesmus quadricauda</i> cultivated in untreated Batik dye wastewater, treated Batik dye wastewater and control (distilled water) containing Bold Basal's medium (BBM) composition over a period of 7 days. Cells were cultivated at at 25 °C without agitation under a dark-light cycle, with an irradiance of 40-60 $\mu\text{mol photon m}^{-2}\text{s}^{-1}$.	101

Figure 4.14	Figure 4.14: Survival trend of (A) mosquito larvae; (B) mosquito pupae and (C) mosquito adults in untreated Batik dye wastewater, treated Batik dye wastewater and control (tap water) over a period of 7 days. The organisms were reared at 25 °C and 18:6 light:dark photocycle.	103
Figure 4.15	SEM micrographs of (A) 1 w/v%; (B) 2 w/v%; (C) 3 w/v% and (D) 4 w/v% P(3HB) in CHCl ₃ electrospun at applied voltage and extrusion rate of 15 kV and 40 μL min ⁻¹ respectively.	106
Figure 4.16	Morphological features of 4 w/v% of P(3HB) solution electrospun at various combination of applied voltage and extrusion rate. The resultant films consisted mainly polymer droplets, spheres and some incipient fibers. The absence of continuous fiber formation indicated the occurrence of electro spraying process instead of electrospinning.	108
Figure 4.17	Morphological features of 4 w/v% P(3HB) in CHCl ₃ /DMF mixed solvent (ratio:8:2) electrospun at (A) & (B) 10 kV; (C) & (D) 15 kV and (E) & (F) 30 kV with an extrusion rate of 40 μL min ⁻¹ . Micrographs (G) & (H) are of similar polymer solution electrospun at applied voltage and extrusion rate of 15 kV and 60 μL min ⁻¹ respectively. Ridges and fused fibers are marked by circled area in (F) & (H) respectively.	111
Figure 4.18	SEM micrographs of fibers electrospun from P(3HB)- TiO ₂ with (A) 10 w/w%; (B) 20 w/w%; (C) 30 w/w%; (D) 40 w/w% and (E) 50 w/w% TiO ₂ loading in 4 w/v% of P(3HB). The ratio of CHCl ₃ /DMF ratio used was 8:2. Applied voltage and extrusion rate were fixed at 15 kV and 40 μL min ⁻¹ respectively. The morphology of cast P(3HB)-50 wt% TiO ₂ is shown in (F).	113
Figure 4.19	Variation in average diameter of P(3HB)- TiO ₂ fibers electrospun with varied TiO ₂ loading. The ratio of CHCl ₃ /DMF mixed solvent used was 8:2. The applied voltage and extrusion rate were fixed at 15 kV and 40 μL min ⁻¹ respectively.	114
Figure 4.20	SEM micrographs showing cross sectional view of a 5 layered P(3HB)-50 wt% TiO ₂ nanofibrous film electrospun at applied voltage and extrusion rate of 15 kV and 40 μL min ⁻¹ respectively in (A) 50 × and (B) 500 × magnifications. The ratio of CHCl ₃ /DMF used was 8:2. The morphology of the fibrous network from a tilted angle of 45 °C is shown in (C).	116

Figure 4.21	Effect of CHCl ₃ /DMF mixed solvent ratio of (A) & (B) 10:0; (C) 9:1; (D) 8:2; (E) 7:3 and (F) 6:4 on the resultant P(3HB)-50 wt% TiO ₂ electrospun fibers. The P(3HB) polymer concentration used was 4 w/v%. Applied voltage and extrusion rate were fixed at 15 kV and 40 μL min ⁻¹ respectively.	118
Figure 4.22	Variation in average diameter of P(3HB)-50 wt% TiO ₂ fibers electrospun at different ratios of CHCl ₃ /DMF mixed solvent. The applied voltage and extrusion rate were fixed at 15 kV and 40 μL min ⁻¹ respectively.	119
Figure 4.23	Morphological features of P(3HB)-50 wt% TiO ₂ fibers electrospun from CHCl ₃ /DMF mixed solvent (ratio=8:2) at (A) 15 kV; (B) 20 kV; (C) 25 kV and (D) 30 kV with an extrusion rate of 40 μL min ⁻¹ . The P(3HB) polymer concentration used was 4 w/v%.	121
Figure 4.24	Fiber diameter distribution of P(3HB)-50 wt% TiO ₂ fibers electrospun from CHCl ₃ /DMF mixed solvent (ratio=8:2) at (A) 15 kV; (B) 20 kV; (C) 25 kV and (D) 30 kV with an extrusion rate of 40 μL min ⁻¹ .	122
Figure 4.25	The decolorization percentage of MG (30 μM) via adsorption process over time using cast and electrospun P(3HB) and P(3HB)-50 wt% TiO ₂ film. The experiment was conducted in triplicates in dark at room temperature (25 °C).	126
Figure 4.26	The decolorization percentage of MG (30 μM) over time using cast and electrospun P(3HB) and P(3HB)-50 wt% TiO ₂ film under (A) sunlight; (B) UV light and (C) fluorescent light.	128
Figure 4.27	COD reduction in MG solution over time via photocatalytic degradation using electrospun P(3HB)-50 wt% TiO ₂ film under solar irradiation. Decolorization experiments were carried out for 2 h with a solar intensity range of 90,400-90,800 Lux.	132
Figure 4.28	Survival trend of <i>Aedes aegypti</i> during stages of (A) larvae; (B) pupae and (C) adult mosquito in untreated MG, treated MG solution and control (tap water) over a period of 14 days. The organisms were reared at 25 °C and 18:6 light:dark photocycle.	134
Figure 4.29	The decolorization percentage of MG in ten repeated decolorization experiments using the same electrospun and cast P(3HB)-50 wt% TiO ₂ films under solar irradiation. Each decolorization experiment was carried out for 2 h. The solar light intensity during the experiments was in the range of	136

90,000-110,000 Lux.

Figure 4.30 SEM micrographs showing morphological features of (A) cast P(3HB)-50 wt% TiO₂ and (C) electrospun P(3HB)-50 wt% TiO₂ before photocatalytic decolorization experiment and (B) cast P(3HB)-50 wt% TiO₂ and (D) electrospun P(3HB)-50 wt% TiO₂ after ten consequent decolorization experiments under solar irradiation. 137

Figure 4.31 Survival curve of *E. coli* JM 109 over exposure time to cast and electrospun P(3HB)-50 wt% TiO₂ films under different illumination sources. The initial cell concentration used was 3.6 X 10⁸ CFU mL⁻¹. Bacterial suspension was sampled at 3 h intervals for 12 h. The samples were spread plated on LB agar and incubated at 37 °C for 24 h. 141

5.0 Discussion

Figure 5.1 Schematics showing the proposed mechanism involved in the MG dye molecules adsorption onto electrospun (A) P(3HB) and (B) P(3HB)-50 wt% TiO₂ film. The electrospun P(3HB) film holds more adsorptive sites for the adsorption of MG molecules via hydrophobic or simple Van der Waals interaction. The charge repulsion between TiO₂ and MG molecules reduces the adsorption of MG on electrospun P(3HB)-50 wt% TiO₂ film. 178

LIST OF PLATES

	Pages
4.0 Results	
Plate 4.1	95
Changes in the physical appearance of 0.4 g P(3HB)-40 wt% TiO ₂ film after (A) first; (B) second; (C) third; (D) fourth; (E) fifth and (F) sixth repeated usages in decolorization experiment. Each decolorization experiment was carried out for 3 h. The solar light intensity during the multiple experiments was in the range of 89,000-110,000 Lux.	
Plate 4.2	130
Digital images of (A & B) cast P(3HB)-50 wt% TiO ₂ ; (C & D) electrospun P(3HB)-50 wt% TiO ₂ ; (E & F) cast P(3HB) and (G & H) electrospun P(3HB) films before and after 2 h of photocatalytic decolorization of MG under sunlight respectively.	

LIST OF ABBREVIATIONS

3HB	- 3-hydroxybutyrate
3HHx	- 3-hydroxyhexanoate
3HV	- 3-hydroxyvalerate
Abs	- Absorbance
ANOVA	- One-way analysis of variance
AOP	- Advanced oxidation process
BBM	- Bold's Basal Medium
CFU	- Colony forming unit
CHCl ₃	- Chloroform
CME	- Caprylate methyl ester
COD	- Chemical oxygen demand
d_j	- Diameter of straight jet end
DMF	- Dimethylformamide
DO	- Dissolved oxygen
EDX	- Energy dispersive X-ray
E_j	- Electric field at the end of the straight jet
GC	- Gas chromatography
GPC	- Gel permeation chromatography
H_c	- Height of Taylor cone
HSD	- Honestly Significant Difference
LB	- Luria Bertani
L_j	- Distance from the needle tip to the end of straight jet
MCL	- Medium-chain-length
MM	- Mineral medium
M_n	- Molecular number

M_w	- Molecular weight
M_w/M_n	- Polydispersity
NR	- Nutrient-rich
P(3HB)- <i>co</i> -(HHx)	- Poly(3-hydroxybutyrate- <i>co</i> -3-hydroxyhexanoate)
P(3HB)- <i>co</i> -(HV)	- Poly(3-hydroxybutyrate- <i>co</i> -3-hydroxyvalerate)
P(3HB)	- Poly(3-hydroxybutyrate)
PE	- Polyethylene
PF	- Pyridinium formate
PHA	- Polyhydroxyalkanoate
PhaA	- 3-ketothiolase
PhaB	- NADPH-dependent acetoacetyl-CoA reductase
PhaC	- PHA synthase
<i>phaC</i>	- PHA synthase gene
PKO	- Palm kernel oil
PLLA	- Poly(L-lactide)
PS	- Polystyrene
PTFE	- Polytetrafluoroethylene
PVC	- Polyvinylchloride
ROS	- Reactive oxygen species
rpm	- Revolution per minute
SCL	- Short-chain-length
SEM	- Scanning electron microscope
THF	- Tetrahydrofuran
TiO ₂	- Titanium dioxide
TSS	- Total suspended solid
UV	- Ultraviolet
v/v	- Volume per volume

FABRIKASI, PENCIRIAN DAN APLIKASI BAHAN NANOKOMPOSIT POLIHIDROKSIBUTIRAT-TITANIUM DIOKSIDA

ABSTRAK

Keperluan yang serius untuk satu kaedah yang berkesan, kos rendah dan mesra alam untuk merawat bahan pencemar pewarna yang dikeluarkan oleh industri tekstil telah mendorong penyelidikan ini. Keupayaan poli-3-hidroksibutirat [P(3HB)] yang boleh terbiodegradasikan untuk menyerap pewarna tekstil dan kemampuan degradasi fotokatalitik titanium dioksida (TiO_2) dieksploitasi untuk merekabentuk sebuah filem nanokomposit yang mempunyai pelbagai fungsi melalui kaedah pengacuan pelarut dan pemintalan elektro. Degradasi bahan pilihan, filem P(3HB) yang dibentuk menggunakan kaedah pengacuan pelarut diuji terlebih dahulu dan disahkan setanding dengan filem ko-polimernya; poli(3-hidroksibutirat-co-5 mol% 3-hidroksivalerat) [P(3HB-co-5 mol % 3HV)] dan poli(3-hidroksibutirat-co-5 mol% 3-hidroksiheksanoat) [P(3HB-co-5 mol% 3HHx)]. Penurunan berat filem-filem ini hampir lengkap dalam lingkungan 8 minggu dalam sedimen bakau tropika. Filem nanokomposit juga melalui degradasi walaupun pada tahap yang lebih rendah disebabkan kesan penyahaktifan mikrob oleh TiO_2 . Kandungan optimum P(3HB) dan TiO_2 dalam filem yang diacu didapati 0.4 g dan 40 wt% masing-masing. Filem ini mempunyai taburan TiO_2 yang serata apabila P(3HB) dan TiO_2 dicampur serentak dalam kloroform diikuti oleh pengacuan selama 24 j. Filem ini berupaya menyahwarna and menyahtoksik sepenuhnya sisa pewarna dari air kumbahan sebenar industri Batik dalam masa 3 j dan mengurangkan keperluan oksigen kimia (COD) sebanyak 80%. Filem 0.4 g P(3HB)-40 wt% TiO_2 menunjukkan kestabilan yang baik dengan peratusan penyahwarna sebanyak $\geq 80\%$ walaupun selepas diguna semula sebanyak enam kali. Air kumbahan pewarna Batik yang telah

dinyahwarna menunjukkan ketiadaan kesan toksik terhadap larva nyamuk, *Aedes aegypti* dan mikroalga, *Scenedesmus quadricauda*. Gentian P(3HB)-TiO₂ yang dielektropintal dari bahan pelarut CHCl₃/DMF (8:2) menunjukkan peningkatan aktiviti fotokatalisis. Kandungan maksimum TiO₂ di dalam 4 w/v% P(3HB) didapati mencapai 50 wt%. Pembekalan voltan dan kadar aliran sebanyak 15 kV dan 40 µL min⁻¹ masing-masing mampu menghasilkan gentian P(3HB)-50 wt% TiO₂ yang homogen dengan diameter purata sebanyak 780 nm. Dalam ketiadaan sumber cahaya, filem P(3HB) elektropintal mampu mempamerkan keupayaan yang tinggi untuk menyahwarnakan (78%) 30 µM Malachite Green (MG) melalui penyerapan sahaja sedangkan nilai yang sepadan untuk filem P(3HB) yang diacu hanya 24%. Filem P(3HB)-50 wt% TiO₂ elektropintal berjaya menyahwarnakan MG sepenuhnya dalam masa 45 min di bawah sinar matahari dengan penyingkiran COD sebanyak 58.7%. Larutan MG yang dirawat dengan cara ini didapati tidak toksik terhadap larva *A. aegypti*. Filem ini mengekalkan kestabilan fotokatalisis yang lebih tinggi berbanding filem yang diacu yang sepadan dengannya. Ia juga dapat diguna semula sekurang-kurangnya 10 kali dengan keupayaan penyahwarnaan ≥98%. Di samping itu, filem ini menunjukkan sifat anti-bakteria yang berkesan terhadap *Escherichia coli* di bawah pencahayaan UVA dengan 1-2 darjah magnitud lebih tinggi daripada filem P(3HB)-50 wt% TiO₂ yang diacu. Satu kaedah yang berkesan, murah, selamat dan yang boleh diguna semula untuk penyahwarnaan, degradasi, penyahtoksikan dan pembasmian kuman daripada air sisa pewarna tekstil telah berjaya direka menerusi penyelidikan ini.

FABRICATION, CHARACTERIZATION AND APPLICATION OF POLYHYDROXYBUTYRATE-TITANIUM DIOXIDE NANOCOMPOSITE

MATERIALS

ABSTRACT

A serious need for a robust, low-cost and eco-friendly method to treat dye pollutants released by textile industries motivated this research. The dye adsorption effect of biodegradable poly-3-hydroxybutyrate [P(3HB)] and the photocatalytic degradation ability of inert titanium dioxide (TiO_2) was exploited to fabricate a multifunctional nanocomposite film via solvent casting and electrospinning. The environmental degradation of the choice material, cast P(3HB) was first tested and confirmed to be comparable to its co-polymers; poly(3-hydroxybutyrate-co-5 mol% 3-hydroxyvalerate) [P(3HB-co-5 mol% 3HV)] and poly(3-hydroxybutyrate-co-5 mol% 3-hydroxyhexanoate) [P(3HB-co-5 mol% 3HHx)]. The weight loss was almost complete by 8 weeks in tropical mangrove sediment. The nanocomposite film was also degradable although to a lesser extent despite the microbial inactivation effect of TiO_2 . The optimum amount of P(3HB) and TiO_2 loading in cast film was found to be 0.4 g and 40 wt% respectively. This film had an even distribution of TiO_2 when mixed concurrently in chloroform followed by stirring for 24 h. It completely decolorized and detoxified real industrial Batik dye wastewater in 3 h and induced a chemical oxygen demand (COD) reduction of 80%. The 0.4 g P(3HB)-40 wt% TiO_2 film exhibited good stability with decolorization percentage of $\geq 80\%$ even after the sixth repeated usage. The decolorized Batik dye wastewater had no toxic effects on mosquito larvae, *Aedes aegypti* and microalgae, *Scenedesmus quadricauda*. Novel P(3HB)- TiO_2 ultrathin fibers electrospun from CHCl_3/DMF

(8:2) mixed solvent showed enhanced photocatalytic activity. The maximum TiO₂ loading in 4 w/v% P(3HB) was 50 wt%. Applied voltage and extrusion rate of 15 kV and 40 $\mu\text{L min}^{-1}$ respectively produced homogeneous P(3HB)-50 wt% TiO₂ fibers with mean diameter of 780 nm. Interestingly, in the absence of irradiation, electrospun (3HB) film exhibited superior ability in decolorizing (78%) 30 μM Malachite Green (MG) via adsorption alone whereas the corresponding value of cast P(3HB) was only 24%. The electrospun P(3HB)-50 wt% TiO₂ completely decolorized MG in 45 min under solar irradiation, which corresponded to 58.7% COD removal. MG solution treated this way was non-toxic against *A. aegypti* larvae. This film retained higher photocatalytic stability than its cast counterpart. It was re-applicable for at least 10 times with $\geq 98\%$ decolorization efficiency. It also showed efficient bactericidal effect against *Escherichia coli* under UVA illumination with 1-2 orders of magnitude more than the cast P(3HB)-50 wt% TiO₂. An effective, inexpensive, safe and reusable method for decolorization, mineralization, detoxification and disinfection of textile dye wastewaters was successfully developed in this research.

1.0 INTRODUCTION

Contamination of natural waters by dyestuff has been a major threat to living organisms throughout the world. Synthetic dyes are used extensively in various applications, especially in the textile dyeing industry. Over 7×10^5 tons of these dyes are produced annually worldwide, while 10–15% of the dyes are lost in the dye effluent during synthesis and processing (Zollinger, 1987; Marungrueng and Pavasant, 2006; Teh and Mohamed, 2011). The wastewater from textile industry contains high amounts of colored organic compounds (Khataee *et al.*, 2009). These substances are reported to have toxic, carcinogenic and mutagenic nature which poses great danger to aquatic systems and human health (Stylidi *et al.*, 2003). One of the best known textile industries in Southeast Asia is the Batik industry. This industry is expanding, especially in countries such as Indonesia, Malaysia and Thailand where Batik is considered a national art form. It is also an important source of employment and locally generated revenue. This industry is usually operated in small scale by workshops and factories throughout the country without a regulated waste disposal system. The textile dye effluent resulting from Batik making process is usually discarded directly into the waterways, prompting both pollution and toxicological concerns.

Apart from textile industry, dye containing effluents are also released into waterways by paper industry, leather tanning industry, food processing and hair colorings (Teh and Mohamed, 2011). Very often, these effluents contain highly toxic dye components. One such controversial dye is the triphenylmethane dye, Malachite Green (MG). MG has been used extensively as a food coloring additive and in the leather, paper, cotton and jute dyeing processes. It is also used as an antifungal and antiprotozoan agent in fisheries and aquaculture industry (Daneshwar

et al., 2007; Goff and Wood, 2008). However, MG and its metabolites are known to cause mutagenic, carcinogenic and teratogenic effects to living organisms (Srivastava *et al.*, 2004). Despite its ban in several countries, its usage is still wide in large parts of the world due to its availability, low-cost and efficacy. Therefore it is crucial to completely remove this dye pollutant from the industrial effluents before entering the aquatic system.

There is a serious need for a robust, low-cost and eco-friendly method to treat the aforementioned contaminants. However, existing wastewater treatment methods do not provide a comprehensive solution for treating dye wastewater and have various limitations. Chemical methods like flocculation and coagulation are not suitable for highly soluble dyes whereas physical methods such as reverse osmosis and ultra-filtration incur high operating costs and cause sludge formation. Biological treatment on the other hand, requires a longer treatment time (Molinari *et al.*, 2004; Bratby, 2006; Ao *et al.*, 2007; Ahmad and Alrozi, 2011). In comparison, adsorption has gained much popularity in treating dye effluents due to its low cost, simple design and ease of operation (Baek *et al.*, 2010). To date, various low cost adsorbents have been tested to decolorize dye wastewater which includes saw dust (Gong *et al.*, 2006), chitosan beads (Becki *et al.*, 2008), silica (Samiey ad Toosi, 2010), coffee beans (Baek *et al.*, 2010), rambutan peel-based activated-carbon (Ahmad and Alrozi, 2011) and polymers (Sekhar *et al.*, 2009; Malana *et al.*, 2010).

Polyhydroxyalkanoate (PHA) is a biodegradable polymer that has gained much commercial interest over the years due to its thermoplastic, nontoxic and renewable nature (Valappil *et al.*, 2008). PHAs are stored intracellularly as energy storage inclusions by various bacteria during environmental stress (Kessler and Witholt, 2004; Sudesh *et al.*, 2004; Lakshman and Shamala, 2006; Suriyamongkol *et*

al., 2007; Valappil *et al.*, 2007; Shah *et al.*, 2008; Sudesh and Iwata, 2008; Pijuan *et al.*, 2009). Of all the known PHAs, poly-3-hydroxybutyrate [P(3HB)] is the most common and widely studied. This highly crystalline polymer is synthesized by a large number of Gram-negative and Gram-positive bacteria (Manna and Paul, 2000; Tokiwa and Ugwu, 2007). In line with the ability of P(3HB) to absorb oil (Sudesh *et al.*, 2007), it was hypothesized that it might also possess the ability to form physical adsorption with dye molecules via hydrophobic interaction or simple Van der Waals. Preliminary investigations of this research proved this hypothesis to be true. Cast P(3HB) film was found to adsorb standard dyes such as Methylene Blue and Rose Bengale. This intrigued the study on the dye adsorption capacity of P(3HB) film. Although adsorption is an efficient method for dye effluent treatment, it merely transfers the dye molecules from its aqueous phase to a solid phase and generates secondary pollution (Prado and Costa, 2009). Alternatively, advanced oxidation process (AOP) based on heterogeneous photocatalysis employing titanium dioxide (TiO₂) and ultraviolet light has been a more promising method in treating dyestuffs (Yeber *et al.*, 2000). TiO₂ is a feasible photocatalyst as it is able to oxidize various organic pollutants, non-toxic, chemically stable, inexpensive and also commercially available (Yu *et al.*, 2002; Ao *et al.*, 2003; Ao *et al.*, 2004; Konstantinou and Albanis, 2004). When TiO₂ is suspended in water and irradiated with UV spectrum from the sunlight or fluorescent light, free radicals such as hydroxyl radicals and superoxide radicals are generated (Hoffman *et al.*, 1995; Fujishima *et al.*, 2000; Essawy *et al.*, 2008; Wu and Yu, 2009). This process is initiated by the excitation of an electron from the valence band to the conduction band forming a hole-electron pair when the TiO₂ particles absorb a light photon that is more energetic than its bandgap (Gouvea *et al.*, 2000; Sauer *et al.*, 2002). The free radicals can oxidize and

mineralize organic materials and kill bacteria (Malato *et al.*, 2009; Teh and Mohamed, 2011).

Though TiO₂ serves these purposes best in its free suspension form, additional cost and time incurred by the separation of the photocatalysts from the treatment system is a major setback (Meyer *et al.*, 2004). Additionally, TiO₂ particles tend to agglomerate in aqueous suspension which reduces the available surface active sites for catalytic activity (Sauer *et al.*, 2002). Thus, more attention is now given to TiO₂ supported on inert and stationary surfaces such as stainless steel (Georgieva *et al.*, 2006), glass (Khataee *et al.*, 2009) and polymers (Birnie *et al.*, 2006; Kasanen *et al.*, 2009). Attempts to immobilize TiO₂ on different supporting materials need to fulfill some requirements; ease of preparation, reusability with retained TiO₂ photoactivity and eco-friendliness. As such, P(3HB) could be used as a suitable solid support to immobilize the catalyst while adding synergism to the overall decolorization process via its adsorption mechanism. Thus, the incorporation of TiO₂ photocatalysts into the P(3HB) matrix via solvent-casting to form a film with dual treatment capability, i.e., adsorption and photocatalytic oxidation was attempted for the first time in this research. Photocatalytic degradation of the adsorbate via advanced oxidation process could offer a complete solution for the removal and breakdown of dye pollutants for a more effective treatment. Moreover, this would also be a cost-cutting approach in TiO₂ mediated dye treatment system as additional step for catalyst recovery is needless and re-applicability of the treatment system becomes feasible.

It is evident from previous studies that the surface area of adsorbent plays a key role in determining the degree of adsorption (Akmil-Basar *et al.*, 2005; Baldez *et al.*, 2008). In addition, photocatalytic activity could also be enhanced by

increasing the available surface active sites of the photocatalyst. Therefore it was hypothesized that higher rate of decolorization could be attained by utilizing electrospinning technique to fabricate ultrafine P(3HB)-TiO₂ fibers with high surface area to volume ratio. Electrospinning generates ultrathin fibers when an electric field is applied to overcome the surface tension of a drop of polymer solution. A variety of fiber morphology and diameter could be obtained via this technique. However, a very narrow processing window is involved in order to obtain the desired homogeneous fibrous structures (Huang *et al.*, 2003; Tan and Obendorf, 2007; Chen *et al.*, 2008). Thus, the optimization of process and system parameters for the fabrication of P(3HB)-TiO₂ nanocomposite fibers were investigated. However, prior to these studies, the environmental degradation of P(3HB) and P(3HB)-TiO₂ film was first investigated as this information was necessary to prove the concept of making an eco-friendly solution for dye wastewater treatment. In brief, the findings of this research are aimed to help in the development of a novel, simple, effective, inexpensive and reusable method for treatment of textile dye wastewaters.

1.1 Research objectives:

The primary goal of this study is to develop a P(3HB)-TiO₂ based nanocomposite film with the combined effect of adsorption and heterogeneous photocatalysis for the decolorization, mineralization and detoxification of dye wastewater which involves a series of objectives as follow:

- 1) To assess the degradability of P(3HB) and P(3HB)-TiO₂ nanocomposite film alongside some commercially important bioplastics; poly(3-hydroxybutyrate-

co-5 mol% 3-hydroxyvalerate) [P(3HB-*co*-5 mol% 3HV)] and poly(3-hydroxybutyrate-*co*-5 mol% 3-hydroxyhexanoate) [P(3HB-*co*-5 mol% 3HHx)] in a tropical mangrove ecosystem.

- 2) To determine the process and system parameters for the fabrication of cast P(3HB)-TiO₂ nanocomposite film.
- 3) To evaluate the solar photocatalytic decolorization, degradation, detoxification and reusability of cast P(3HB)-TiO₂ nanocomposite film on real industrial Batik dye wastewater.
- 4) To determine the process and system parameters for the fabrication of ultrathin P(3HB)-TiO₂ nanocomposite fibers via electrospinning.
- 5) To compare the performance of cast and electrospun P(3HB) and P(3HB)-TiO₂ films in decolorizing a controversial dye, Malachite Green via adsorption and photocatalytic degradation.
- 6) To compare the photocatalytic stability and antibacterial activity of cast and electrospun P(3HB)-TiO₂ nanocomposite films.

2.0 LITERATURE REVIEW

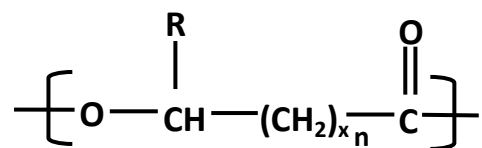
2.1 Overview of polyhydroxyalkanoate (PHA)

Polyhydroxyalkanoates (PHAs) are biopolyesters of various hydroxyalkanoates (HAs) synthesized as intracellular carbon and energy storage compounds by numerous bacteria (Lee and Choi, 1999; Tang *et al.*, 2008; Sudesh *et al.*, 2011). Gram-positive and gram negative bacteria from at least 75 different genera are known to synthesize PHA (Reddy *et al.*, 2003). These intracellular reserve polymers are accumulated up to a maximum of 90% of the cell dry weight (Abe *et al.*, 2001) during nutrient stress which includes limitation of nitrogen, phosphorus, magnesium or oxygen in the presence of excess carbon supply (Anderson and Dawes, 1990; Doi *et al.*, 1990; Kato *et al.*, 1996; Madison and Huisman, 1999). The assimilated carbon sources are biochemically processed into 3-hydroxyalkanoic acid (3HA) monomer units and polymerized into water insoluble inclusions in the microbial cell cytoplasm.

The high refractivity of PHA granules allows it to be observed under phase contrast microscope as discrete inclusions of 0.2-0.5 μm in diameter (Sudesh *et al.*, 2000; Sathesh and Murugesan, 2010). Bacterially produced PHAs have adequately high molecular mass to match the polymer qualities of conventional plastics such as polyethylene (PE) and polypropylene (PP) (Madison and Huisman, 1999; Qin *et al.*, 2007). This has drawn increasing attention on PHA as a substitute for petrochemical-based synthetic plastics as it can be thermally processed into various applications. PHAs are also advantageous over conventional plastics due to its biodegradability in natural environments (Sudesh and Iwata, 2008). In addition, the use of renewable resources such as sucrose, starch, cellulose, triacylglycerols, palm

oil and activated sludge to supply microorganisms with various carbon substrates for the synthesis of PHA is an added plus (Reddy *et al.*, 2003; Ojumu *et al.*, 2004).

Since the identification of poly(3-hydroxybutyric acid) (P[3HB]) in *Bacillus megaterium* by Lemoigne (1926), 3-hydroxybutyrate (3HB) was regarded as the sole PHA monomeric unit. The presence of other monomer units such as 3-hydroxyvalerate (3HV) and 3-hydroxyhexanoate (3HHx) was only discovered almost 50 years later by Wallen and Rohwedder (1974). Thus far, more than 150 different monomer constituents of PHA have been identified (Rehm *et al.*, 2003; Steinbüchel and Lutke, 2003). Bacterial PHA can be divided into three main types depending on the number of carbon atoms in the monomeric units: short-chain-length (scl), medium-chain-length (mcl) and a combination of scl-mcl. The scl-PHAs consist of 3 to 5 carbon atoms, mcl-PHAs have 6 to 14 carbon atoms whereas the number of carbon atoms in scl-mcl-PHAs can range from 3 to 14 per molecule (Li *et al.*, 2007). While the homopolymer, P(3HB) is the most widely studied scl-PHA, its copolymers containing 3-hydroxyvalerate (HV), 3-hydroxyhexanoate (HHx) or 4-hydroxybutyrate (4HB) monomers are also synthesized (Figure 2.1). In nature, scl-PHAs containing mainly 3HB units or mcl-PHAs containing 3-hydroxyoctanoate (HO) and 3-hydroxydecanoate (HD) are produced as the major monomers by most of the microbes (Anderson and Dawes, 1990; Lee, 1996; Steinbüchel & Fächtenbusch, 1998). These copolymers can be more flexible and tougher plastics as compared to the relatively stiff and brittle P(3HB). The usually elastomeric and sticky mcl-PHAs can be even modified to make rubbers (Suriamongkol *et al.*, 2007).



Number of repeating units, n	Alkyl group, R	Polymer type
1	Hydrogen	Poly(3-hydroxypropionate)
	Methyl	Poly(3-hydroxybutyrate)
	Ethyl	Poly(3-hydroxyvalerate)
	Propyl	Poly(3-hydroxyhexanoate)
	Pentyl	Poly(3-hydroxyoctanoate)
	Nonyl	Poly(3-hydroxydodecanoate)
2	Hydrogen	Poly(4-hydroxybutyrate)
3	Hydrogen	Poly(5-hydroxyvalerate)

Figure 2.1: General structures of polyhydroxyalkanoates (Lee, 1996).

2.2 PHA biosynthesis

PHA synthase (PhaC) is the key enzyme responsible for the polymerization of (*R*)-3HA monomers (Pantazaki *et al.*, 2003; Qin *et al.*, 2007). Owing to the stereospecificity of this enzyme, all the 3HA monomer units are in the *R* configuration (Dawes and Senior, 1973; Sudesh *et al.*, 2000). PHA synthase are differentiated based on their subunit composition, substrate specificity and primary structure (Sheu and Lee, 2004; Potter and Steinbuchel, 2006; Taguchi and Tsuge, 2008). PHA synthases of class I and II are represented by PHA synthase of *Cupriavidus necator* and *Pseudomonas aeruginosa* respectively. The class I synthase consists of a single subunit (PhaC) with preference towards scl-HA monomers. However, PHA synthases of *Aeromonas caviae* and *Rhodospirillum rubrum* that belong to this class of enzymes do also incorporate 3HHx monomers. On the other hand, the class II synthases have two similar subunits (PhaC1 and PhaC2) which actively polymerize mcl-HA monomers (Sudesh *et al.*, 2000; Jendrosek, 2009). The class III PHA synthases represented by *Chromatium vinosum* has two different subunits (PhaC/PhaE) which generally prefer to utilize scl-HA monomers (Yuan *et al.*, 2001). PHA synthases of *Bacillus megaterium* having two subunits (PhaC/PhaR) represent class IV of the synthase enzyme and show substrate preference similar to class III PHA synthase (McCool and Canon, 2001). The nature of this enzyme together with the kind of carbon sources fed to the microorganism and its active metabolic pathway determine the type of PHA produced (Sudesh and Doi, 2005).

The route for P(3HB) synthesis in *C. necator* is one of the simplest and extensively studied PHA biosynthetic pathway (Figure 2.2). Via this route, β -ketothiolase (PhaA) condenses two molecules of acetyl-CoA to form acetoacetyl-

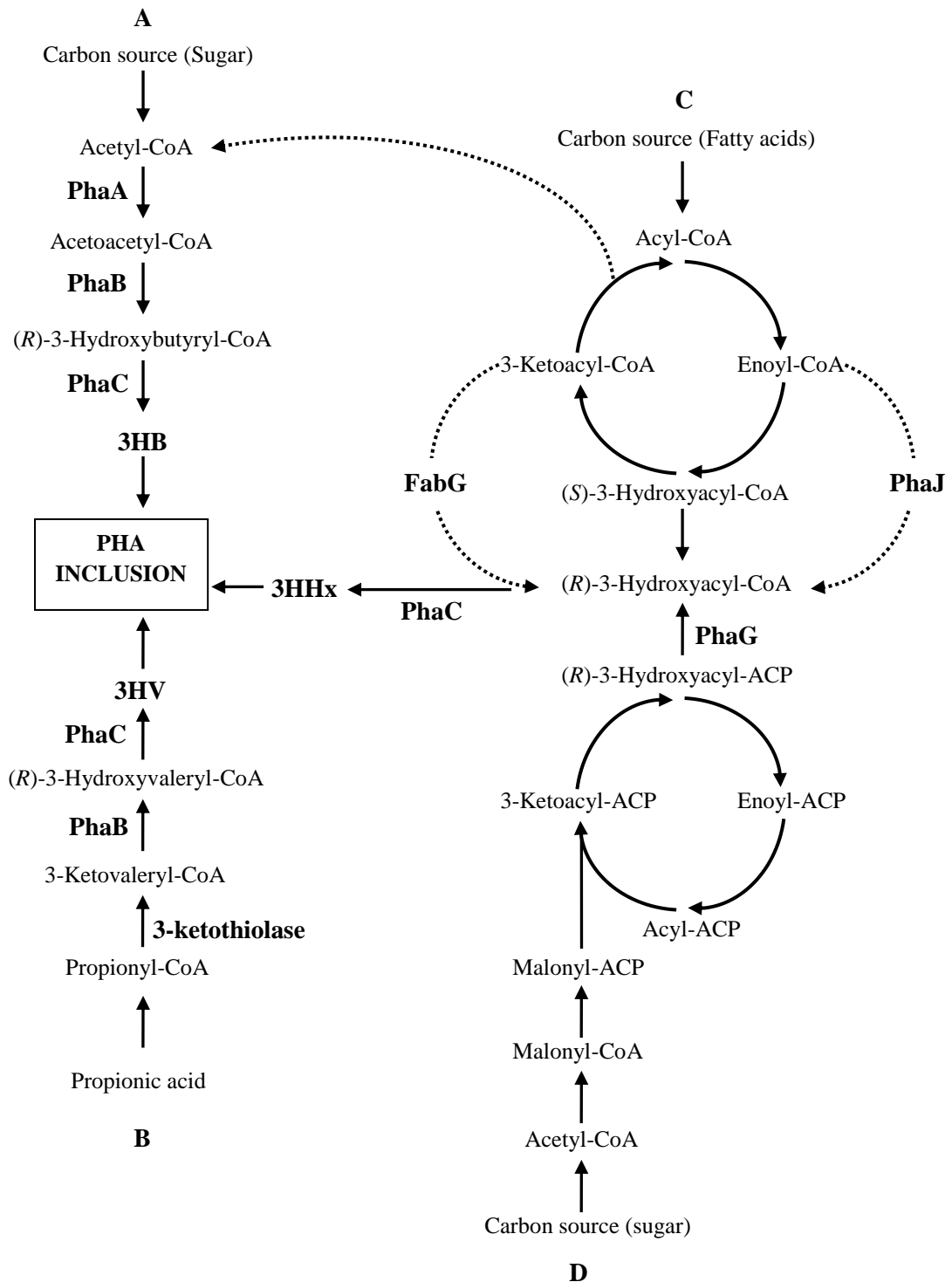


Figure 2.2: Biosynthesis pathway of (A) P(3HB); (B) P(3HB)-*co*-(3HV); (C) P(3HB)-*co*-(3HHx) via fatty acid β -oxidation and (D) P(3HB)-*co*-(3HHx) via fatty acid *de novo* synthesis. PhaA, β -ketothiolase; PhaB, NADPH dependent acetoacetyl-CoA reductase; PhaC, PHA synthase; PhaG, 3-hydroxyl-ACP-CoA transferase; PhaJ, (*R*)-enoyl-CoA hydratase; FabG, 3-ketoacyl-CoA reductase (Sudesh *et al.*, 2000).

CoA. An NADH₂ dependent acetoacetyl-CoA reductase (PhaB) then catalyzes the conversion of acetoacetyl-CoA to (*R*)-3-hydroxybutyryl-CoA. The PhaC then catalyzes the polymerization of (*R*)-3-hydroxybutyryl-CoA monomers into P(3HB) polymer (Sudesh *et al.*, 2000; Khanna & Srivastava, 2005; Suriamongkol *et al.*, 2007). According to Anderson *et al.* (1990), all of the three enzymes involved in P(3HB) synthesis are to be found in the cytosol of the cell where PHB accumulation occurs. Variations in the carbon sources fed to bacteria including *C. necator* can give rise to the synthesis of PHAs with different C3 to C5 monomers (Steinbüchel and Schlegel, 1991; Dias *et al.*, 2006). For instance, a random copolymer composed of HB and HV [P(3HB-*co*-3HV)] can be obtained by adding propionic acid in glucose media. In this biosynthetic pathway, 3-ketothiolase mediates the condensation of propionyl-CoA with acetyl-CoA into 3-ketovaleryl-CoA which is then reduced to (*R*)-3-hydroxyvaleryl-CoA (Figure 2.2). PhaB and PhaC involved in PHB synthesis then catalyzes the polymerization of P(3HB-*co*-3HV) copolymers (Poirier, 2002). The addition of aliphatic fatty acids with an odd number of carbon atoms such as valeric, heptanoic and nonanoic acids can increase the fraction of 3HV in P(3HB-*co*-3HV) (Steinbüchel and Lütke-Eversloh, 2003). *A. caviae* (Doi *et al.*, 1995) and *Aeromonas hydrophila* (Chen *et al.*, 2001; Han *et al.*, 2004) are capable of naturally synthesizing P(3HB-*co*-3HHx) when fed with fatty acids with even number of carbons. The enoyl-CoA hydratase (PhaJ) enzyme in these strains catalyzes (*R*)-specific hydration of 2-enoyl-CoA to supply (*R*)-3-hydroxyacyl-CoAs for the polymerization of P(3HB-*co*-3HHx) synthesis via the fatty acid *de novo* biosynthesis or fatty acid β -oxidation pathway (Fukui and Doi, 1997; Tsuge *et al.*, 2003).

2.3 Poly(3-hydroxybutyrate), (3HB)

P(3HB) is the best characterized and most extensively studied of all the known PHAs. In its native granule, P(3HB) exists in amorphous (Barnard and Sanders, 1989; Amor, 1991) state while extracted granules have 55–80% crystallinity (Holmes, 1988). The weight-average molecular weight (M_w) of P(3HB) produced from wild-type bacteria is usually in the range of 1×10^4 to 3×10^6 g/mol. The densities of amorphous and crystalline P(3HB) are 1.18 and 1.26 g/cm³, respectively (Doi, 1990; Sudesh and Abe, 2010). The mechanical properties of P(3HB) in terms of Young's Modulus (3.5 GPa) and tensile strength (43 MPa) is comparable to the corresponding values of polypropylene (PP). However, the elongation at break of P(3HB) is only 5 % as compared to the 400% value for PP causing the former to be more brittle and stiffer than the latter (Sudesh *et al.*, 2000). The brittleness of the P(3HB) films is due to the formation of large crystalline domains in the form of spherulites (Sudesh and Doi, 2005). However, advances in genetic engineering allows the generation of recombinant bacteria which can produce PHA governed by heterologous genes. A recombinant *Escherichia coli* harboring the PHA synthase gene from *R. eutropha* could produce ultra-high-molecular weight P(3HB) with M_w values of 3×10^6 to 1.1×10^7 and notably improved mechanical properties (Kusaka *et al.*, 1998). The Young's Modulus, tensile strength and elongation to break of the homopolymer were found to be 1.1 GPa, 62 MPa and 58%, respectively (Kusaka *et al.*, 1999).

P(3HB) is 100% biodegradable and has attracted much ecological interests as it can undergo rapid degradation under environmental conditions such as aerobic and anaerobic (Nishida and Tokiwa, 1993) and thermophilic conditions (Calabia and Tokiwa, 2006). Therefore, it can be used to manufacture biodegradable bottles,

films, adhesives and fibers for packaging purposes. It can also be used as a raw material for enantiomerically pure chemicals and paint industry (Williams *et al.*, 1999; Keshavarz and Roy, 2010). Processing window of P(3HB) is very narrow due to its relatively close melting temperature ($T_m=180$ °C) and thermal degradation temperature (200 °C). P(3HB) has good resistance to UV but not durable to acids and bases. It can be dissolved in chloroform or chlorinated hydrocarbons but not water; therefore it is resistant to hydrolytic degradation (Geller, 1996; Sudesh *et al.*, 2000). Due to its biodegradable and biocompatible behaviour, P(3HB)-based polymer or composite have the potential to be used in tissue engineered products such as drug release carrier, implants or medicinal instruments (Williams & Martin, 2002; Amara, 2008; Heydarkhan-Hagvall *et al.*, 2008). Low molecular weight P(3HB) has been found to be a common constituent of the animal cell membranes. The nontoxicity of P(3HB) is also further supported by the fact that a relatively large quantity of low M_w P(3HB) is present in the human blood and that the 3-hydroxybutyric acid (3HB) is an ubiquitous metabolite in all higher living organisms (Werner and Freier, 2006).

Blending of P(3HB) with other polyesters like poly(D,L-lactide-*co*-glycolide) (PLGA) or poly(*p*-dioxanone) does not increase the flexibility of the homopolymer due to its poor miscibility (Werner and Freier, 2006). In order to improve the mechanical properties of P(3HB), it is usually incorporated with other HA (3-14 carbon atom) monomers to form random copolymers in addition to increasing the molecular weight of P(3HB) (Khanna and Srivastava, 2004). However, the production cost of P(3HB) and its copolymers is high and still remains a challenge in matching that of conventional non-biodegradable plastic (Tokiwa and Ugwu, 2007; Castilho *et al.*, 2009). Thus, various attempts are being made to utilize cheap

and renewable carbon source to enable the commercialization and widespread use of these polymers.

2.4 Poly(3-hydroxybutyrate-*co*-3-hydroxyvalerate), P(3HB-*co*-3HV)

The commercialization of P(3HB-*co*-3HV) was started in 1980s under the trade name Biopol™ by Imperial Chemical Industries (ICI). Propionic acid and glucose which serve as the precursor for 3HV and 3HB respectively were used to develop P(3HB-*co*-3HV) random copolymers containing 0-30 mol% of 3HV unit (Holmes, 1981). The isodimorphism of the 3HV and 3HB monomer units causes both units to co-crystallize in either of the polymer crystal lattices (Werner and Freier, 2006; Cheng *et al.*, 2008; Pan and Inoue, 2009). Due to this, the degree of crystallinity of P(3HB-*co*-3HV) remains almost similar to P(3HB) (50–70%) and thus, the quality of the copolymer in general was not significantly improved as compared to the homopolymer with 3HV content up to 20 mol% (Doi and Steinbüchel, 2001; Khanna and Srivastava, 2004). However, the mechanical properties of P(3HB-*co*-3HV) strongly rely on the molar fraction of 3HV. Solution cast films of P(3HB-*co*-3HV) showed decrement in the value of tensile strength and Young's Modulus with an increase of 3HV fraction from 0 to 25 mol%. This suggested the increase in the flexibility of P(3HB-*co*-3HV) films. The toughness of the film was markedly improved as the elongation to break reached 700% when 28 mol% of 3HV was incorporated into P(3HB). On the other hand, the lowering of T_m with increasing 3HV content (0 to 25 mol%) without alteration on the thermal degradation temperature provides more room for thermal processing without

thermally degrading the copolymer (Khanna and Srivastava, 2004; Sudesh and Abe, 2010).

2.5 Poly(3-hydroxybutyrate-co-3-hydroxyhexanoate), P(3HB-co-3HHx)

P(3HB-co-3HHx) possesses improved mechanical property and processability as compared to P(3HB) and P(3HB-co-3HV) (Doi *et al.*, 1995; Matsusaki *et al.*, 2000). Co-polymerization of P(3HB) with HHx monomer unit which has a longer alkyl side-chain avoids isodimorphism as the HB and HHx monomer units could not fit into the crystalline lattices of each other. As the HHx molar fraction is increased from 0 to 25 mol%, the crystallinity of P(3HB-co-3HHx) exhibits decrement from 60 to 18%. The tensile strength of the solution-cast films of P(3HB-co-3HHx) displayed decrement from 43 to 20 MPa while elongation to break increased from 6 to 850% when the HHx content was increased from 0 mol% to 17 mol% (Werner and Freier, 2006; Cheng *et al.*, 2008; Sudesh and Abe, 2010). The nature of P(3HB-co-3HHx) copolymer becomes soft and flexible with increasing HHx fraction. Incorporation of small amounts of 3HHx units (5 mol%) into the 3HB sequence reduces the melting point from 179 °C to less than 155 °C (Doi, 1990; Loo *et al.*, 2005) while further increment in HHx fraction up to 25 mol% results in T_m value of 52 °C. P(3HB-co-3HHx) has also been shown to be suitable candidate for blending in order to improve the ductility of stiff and brittle polyesters (Werner and Freier, 2006).

2.6 Extracellular PHA degradation

Extracellular degradation is the utilization of an exogenous polymer by a not-necessarily PHA accumulating microorganism that secretes extracellular PHA depolymerases, which are carboxyesterases. Native intracellular PHA granules are in the amorphous state whereas the extracellular PHA is partially crystalline. The source of extracellular polymer in environment is PHA released by accumulating cells after death and cell lysis (Jendrosek and Handrick, 2002). Microorganisms excrete extracellular PHA depolymerase as solid PHA polymer of high molecular weight is unable to diffuse through the cell wall of bacteria (Abe *et al.*, 2001). PHA depolymerases hydrolyze water-insoluble PHA into water-soluble products of monomers or oligomers which is then metabolized within cells into CO₂ and H₂O (Sridewi *et al.*, 2006). The rate of biodegradation was found to be influenced by several factors in a given environment such as microbial population, temperature, moisture level, pH and nutrient supply besides the composition, crystallinity, additives and surface area of PHA itself (Abou-Zeid *et al.*, 2001).

Extracellular PHA depolymerases are ubiquitous in the environment (Tokiwa and Calabia, 2004). The earliest discovery of PHA-degrading bacteria belonging to *Bacillus*, *Pseudomonas* and *Streptomyces* was made by Chowdhury (1963). From then onwards, a vast a number of aerobic and anaerobic PHA-degrading bacteria have been isolated from various environments such as soil, sludge and sea-water. Mergaert *et al.* (1993) isolated and identified 295 strains capable of degrading PHB and P(3HB-*co*-3HV) copolymer from soils. Recently, a thermoalkalophilic P(3HB-*co*-3HV) esterase was reported to be produced by the soil isolate *Streptomyces* sp. IN1 (Allen *et al.*, 2011). An extracellular mcl-PHA depolymerase which was purified from *Thermus thermophilus* HB8 has the ability to hydrolyze mcl PHAs and

p-nitrophenyl (*p*NP) esters but not scl PHAs (Papaneophytou *et al.*, 2011). Volova and co-workers isolated several PHA-degrading strains identified as *Enterobacter* sp., *Bacillus* sp. and *Gracilibacillus* while studying the biodegradability of P(3HB) and P(3HB)-*co*-11 mol% 3HV in a tropical marine environment of South China Sea (Volova *et al.*, 2010). Many P(3HB)-degrading fungi have also been identified thus far (Matavulj and Molitoris, 1992; Manna and Paul, 2000; Sang *et al.*, 2001; Shah *et al.*, 2010).

Degradation of PHA films proceeds via surface erosion mechanisms whereby bacteria attaches on the porous area on the film surface and secrete depolymerase enzymes to perform catalytic action on the polymer (Wang *et al.*, 2004). These enzymes go through a two step heterogeneous enzymatic hydrolysis to disintegrate PHA films which includes the adsorption of enzyme on the surface of PHA films by the substrate-binding domain followed by the hydrolysis of PHA molecule by the catalytic domain (Feng *et al.*, 2003). The catalytic domain contains the catalytic machinery composed of a catalytic triad (Ser-His-Asp). The serine is part of a lipase box pentapeptide Gly-X-Ser-X-Gly, which has been found in all known hydrolases such as lipases, esterases and serine proteases. A linker region connects the aforementioned two domains (Jaeger *et al.* 1994). The degradation of different PHA films depends greatly on the specificity of the active site in the catalytic amino acid domain structure of a depolymerase enzyme (Shinomiya *et al.*, 1998; Kasuya *et al.*, 1999). It is also well documented that although this enzyme is able to adhere on various substrate surfaces, but the active site in its catalytic domain is specific for the hydrolysis of PHA molecules (Kasuya *et al.*, 1996).

2.7 Dye wastewater

To date, approximately more than 100,000 commercial dyes are available worldwide with annual production of up to a million tons (Zollinger, 1987; Hunger, 2003; Husain, 2006; Christie, 2007). Almost 15% of the marketed dyes are released into the environment as wastes via manufacturing and processing of these dyes (Husain, 2006; Hai *et al.*, 2007). Some of the biggest consumers of dyes are textile, tannery, paint, dyeing, photography, and paper and pulp industries (Gupta and Suhas, 2009). The textile industry is a prominent economic sector in Malaysia, generating a total profit worth approximately RM18.0 million (US\$ 5.4 million) from manufactured exports in 2007 (Lim *et al.*, 2010). Most of these industries do not adhere to the proper dye waste disposal system due to lack of awareness and as a way to reduce the overall running capital. Hence, dye effluents containing unconsumed dye compounds along with auxiliary compounds added to the dyeing solution such as fixing agents, organic acids, surfactants and diluents are released directly into adjacent water bodies.

Dyes belong to the intolerable group of pollutants due to their high toxicity, color, salinity and chemical oxygen demand (COD) (Combes and Havelandsmith, 1982; Christie, 2007; Bae and Freeman, 2007). In general, human exposure to dyes and their metabolites through skin contact, oral ingestion and inhalation leads to skin and eye irritation, skin sensitization, mutagenicity and carcinogenicity (Hatch and Maibach, 1999; Rai *et al.*, 2005; Christie, 2007). Azo dyes which comprise 65–70% of the total number of dyes produced can be catalyzed into aromatic amines that cause intestinal cancer (Wu, 2009). Besides, dyes also cause aesthetic pollution by adding color to natural waters which is visible to human eye.

In addition, the presence of dye molecules attenuates and reduces transmission of light in water which in return disturbs the biological processes within an aquatic ecosystem (Kuo, 1992; Nasuha and Hameed, 2011). Furthermore, some dyes have the tendency to sequester metal and this may cause microtoxicity to fish and other aquatic organisms (Mondal, 2008; Gupta and Suhas, 2009). As such it is of prime importance to efficiently remove these dye compounds from textile and other dye based effluents prior to their disposal.

2.7.1 Types of dyes

Dyes used preferentially in textile industries ought to possess some basic qualities such as intense coloration, solubility in water, affinity towards textiles and fastness. Textile dyes show high affinity for one or more textile fibers under precise conditions of temperature and with the presence of specific auxiliaries (Choudhury, 2006). Two key components of dye molecules are the chromophores and auxochromes. The former produces color while the latter supplements the chromophores and enables the solubility of dye molecules in water plus enhances its affinity towards the textile fibers. Dyes can be classified based on their chemical structure and the presence of chromophoric such as a major azo linkage, triarylmethane or an anthraquinone unit (Zollinger, 1987; Gupta and Suhas, 2009). Dyes are also distinguishable on the basis of their mode of application and solubility (Hunger, 2003; Parsons, 2004) (Table 2.1). Soluble dyes include acid, direct, basic, mordant, metal complex, and reactive dyes where as insoluble dyes include sulfur, azoic, vat and disperse dyes.

Table 2.1: Classification of dyestuffs

Dyestuffs	Characteristics	Principal chemical classes	Associated use
Acid dyes	Water soluble	Azo (including premetallized), anthraquinone, triphenylmethane, azine, xanthene, nitro and nitroso	Nylon, wool, silk, modified acrylics, and also to some extent for paper, leather, ink-jet printing, food and cosmetics
Cationic dyes	Water soluble dyes that yield coloured cations in solution	Diazahemicyanine, triarylmethane, cyanine, hemicyanine, thiazine, oxazine and acridine	Silk, wool, tannin-mordanted cotton, paper, polyacrylonitrile, modified nylons, modified polyesters, cation dyeable polyethylene terephthalate and to some extent in medicine too
Disperse dyes	Water-insoluble nonionic dyes used for hydrophobic fibers from aqueous dispersion	Azo, anthraquinone, styryl, nitro and benzodifuranone groups	Polyester and to some extent on nylon, cellulose, cellulose acetate, and acrylic fibers
Direct dyes	Water-soluble anionic dyes that have high affinity for cellulosic fibers when dyed from aqueous solution in the presence of electrolytes	Polyazo compounds, along with some stilbenes, phthalocyanines and oxazines	Cotton and rayon, paper, leather, and, to some extent to nylon
Reactive dyes	Bright colored dyes that have simple chemical structures and narrow absorption bands, making them advantageous over direct dyes	Azo, anthraquinone, triarylmethane, phthalocyanine, formazan, oxazine	Cotton and other cellulose, but are also used to a small extent on wool and nylon
Solvent dyes	Solvent soluble (water insoluble) and generally nonpolar or little polar, i.e., lacking polar solubilizing groups such as sulfonic acid, carboxylic acid or quaternary ammonium	Azo and anthraquinone, phthalocyanine and triarylmethane	Plastics, gasoline, lubricants, oils, and waxes
Vat dyes	Water-insoluble dyes	Anthraquinone (including polycyclic quinones) and indigoids	Mainly cotton and as soluble leuco salts to cellulosic fibers and also for rayon and wool

2.8 An outlook on the current wastewater treatment methods

Challenge lies in the treating of dye effluent which often contains a mixture of recalcitrant dye compounds. High efficacy, low cost, simple operation and re-applicability are the most sought after qualities in a dye effluent treatment system. Numerous physical, chemical and biological methods with varying degree of efficiency have been investigated for the remediation of dye effluent to date which includes coagulation/flocculation, filtration, adsorption, biological treatment and advanced oxidation processes. Each of these methods has its advantages and disadvantages as discussed in the following sections.

2.8.1 Coagulation/flocculation

Treatment of dye wastewater via coagulation/flocculation involves the addition of coagulants such as alum, magnesium carbonate, ferrous salt, and clays to the dye effluent to induce flocculation (Kagaya *et al.*, 1999; Cheng *et al.*, 2007). This technique gives satisfactory removal of disperse, sulfur, and vat dyes but not economically feasible due to the use of expensive chemicals. Other drawbacks of this process are the production of concentrated sludge in large quantities and high dependence on pH (Lee *et al.*, 2006; Gupta and Suhas, 2009). Organic coagulants (polymers), mainly, polysaccharides are favored, though more expensive, as they tend to produce less sludge than the inorganic coagulants. Additionally, excessive polymer use has been reported to be toxic to bioassay test organisms (Mishra and Bajpai, 2005). Furthermore, this method is ineffective for treating highly water-soluble dyes (Wu, 2009) and shows poor results in the removal of azo, reactive, acid and especially the basic dyes (Hai *et al.*, 2007).

In a previous study, coagulation was used in conjunction with adsorption to remove direct, mordant and basic dyes. The addition of a small amount of a coagulant polyaluminium chloride (PACl) helped to flocculate powdered activated carbon (PAC) to form PAC-PACl sludge, which settles rapidly, enabling the reuse or disposal of PAC (Sanghi and Bhattacharya, 2003). Over the past years, electro-coagulation has been gaining more interest than the traditional coagulation/flocculation due to its ability to remove small colloidal particles, direct generation by electro-oxidation of a sacrificial anode that avoids the addition of excessive amount of coagulants, simple operation, short reaction time and low sludge production. However, the presence of sizing agents, surfactants, salts, volatile organic compounds and high pH in textile dye wastewaters can interfere with electro-coagulation process and affect its efficiency (Alinsafi *et al.*, 2005).

2.8.2 Filtration

Filtration technology includes microfiltration, ultrafiltration, nanofiltration, and reverse osmosis with each membrane process best suited for a particular water treatment function (Cheremisinoff, 2002; Xue *et al.*, 2008). Among them, microfiltration is the least effective wastewater treatment system due to its large pore size. On the other hand, ultrafiltration and nanofiltration separation techniques are more effective in removing all classes of dyestuffs. Nanofiltration is able to separate relatively small organic molecules (M_w : 200–1000 g/mol) as well as ionic components. Nevertheless, the clogging and fouling of membrane pores are inevitable causing the permeate flux to decline. The clogging or fouling of membranes could be minimized by grafting the filtration membranes with polymers

having functional groups that can repel the dye molecules (Akbari *et al.*, 2002). The high working pressure, substantial energy consumption, expensive membrane and short membrane life are other drawbacks of this method. Reverse osmosis (Marcucci *et al.*, 2001; Al-Bastaki, 2004; Sostar-Turk *et al.*, 2005) is impermeable to almost all dye compounds and thus is effective in decolorizing and desalting dye wastewaters under high working pressure. The most widely used membrane materials in reverse osmosis are cellulose acetate and polyamide (nylon) (Qasim, 1998). The inherent problems in the application of reverse osmosis system are the presence of particulate materials in wastewater, precipitation of soluble salt and physical and chemical makeup of the wastewater which lead to the clogging and accumulation of solute (concentration-polarization) on the membrane surface (Cheremisinoff, 2002).

2.8.3 Adsorption

The adsorption of synthetic dyes on cheap and efficient solid supports is considered as a simple and economical method for the removal of dye from wastewaters (Forgacs *et al.*, 2004). Physical adsorption (physisorption) is referred to the physical attraction between the solid surface and the adsorbed molecules. The attractive forces between adsorbate and adsorbent molecules in physisorption are van der Waals forces which are weak in nature and thus results in reversible adsorption. Conversely, the chemical bonding between the solid surface and the adsorbed molecules (chemisorptions) are higher in strength. In general, a good adsorbent must possess high surface area and the time taken to reach adsorption equilibrium should be as minimal as possible to ensure rapidness in dye removal. Previous studies reveal that activated carbons are efficient and commercially

applicable materials for the removal of dye pollutants but the use is sometimes limited due to its high cost. In addition, the activated carbons become exhausted after their use in wastewater treatment, thus not capable of further dye adsorbance. Therefore, regeneration of activated carbon via thermal, chemical, oxidation or electrochemical method is necessary for allowing its re-applicability (Zhou and Lei, 2005). This additional step adds cost and also results in a loss of carbon which may reduce the adsorption capacity of the treatment system. This prompted the search for low cost alternative adsorbents for dye adsorption process (Ali and Gupta, 2007; Malana *et al.*, 2010). Natural clay is an attractive choice of adsorbent for the removal of dyes from wastewaters due to its low cost. Activated carbons are known to show good affinity towards basic dyes whereas acid dyes show better adsorption on activated clay/bentonite (Sanghi and Bhattacharya, 2003). Wood, saw-dust, fly-ash, coal, silica, fruit peels, spent tea leaves and a variety of other inexpensive adsorbents had been tested and proved useful in decolorizing dye effluents (Gupta and Suhas, 2009).

There has also been increasing interest in the use of biological materials such as peat, yeast, chitosan, fungi and bacterial biomass as biosorbents to concentrate and remove dyes from aqueous solutions. The decolorization by living or dead microbial biomass could be attributed to surface ion-exchange, adsorption, complexation, complexation-chelation and micro-precipitation (Crini, 2006) via the interaction of dye molecules with the functional groups in polysaccharides, proteins and lipids present on cell walls (Srinivasan and Viraraghavan, 2010).